The double-tailed normal-incidence-monochromator beamline at CAMD

Cherice M. Evans
Department of Chemistry, Louisiana State University, Baton Rouge, Louisiana 70803

John D. Scott and Eizi Morikawa[a)]
J. Bennett Johnston Sr. Center for Advanced Microstructures and Devices (CAMD), Louisiana State University, Baton Rouge, Louisiana 70806

(Presented on 23 August 2001)

A high-resolution, high-intensity 3 m normal-incidence-monochromator beamline at the J. Bennett Johnston Sr. Center for Advanced Microstructures and Devices is described. The beamline was designed primarily for high-resolution photoelectron spectroscopy utilizing a Scienta electron analyzer, which is permanently placed as an endstation at the beamline. In order to expand utilization of the beamline, an additional beamline tail also has been designed. Optical design of the beamline and preliminary performance results are discussed. © *2002 American Institute of Physics.* [DOI: 10.1063/1.1445816]

I. INTRODUCTION

The normal-incidence monochromator (NIM) has a relatively long history, many instruments have been constructed and operated successfully at synchrotron light facilities world-wide, dating from the 1960's.[1–13] Recently, NIMs have regained attention because the energy tunability and high-resolution capability in the ultraviolet (UV)-vacuum ultraviolet (VUV) region make them well suited as excitation sources for ultrahigh resolution photoelectron spectroscopy. The 4 m NIM[11] at the Synchrotron Radiation Center in Wisconsin is a representative instrument that delivers tunable monochromatic UV–VUV photons to a Scienta electron analyzer with a resolving power greater than 30 000. In this article, we describe the design and the initial performances of the J. Bennett Johnston Sr. Center for Advanced Microstructures and Devices (CAMD) 3 m NIM beamline, which primarily targets high-resolution photoemission spectroscopy using a Scienta SES-200.

II. OPTICAL DESIGN

In designing the NIM beamline, high resolving power, high-intensity photon flux, and high degree of plane polarization over the range from ~3 to 40 eV were the primary aims. Layout of the 3m-NIM beamline is shown in Fig. 1 and detailed descriptions of optics are summarized in Table I. Details regarding how this design resulted from consideration of the stated requirements in light of coupling the apertures of the source, the monochromator, and the electron analyzer have been published.[14] The water-cooled ellipsoidal mirror (M_0) accepts full 70 mrad of horizontal radiation from a dipole magnet. By using two cylindrical mirrors (M_1 and M_2), each producing the same coma but oppositely signed in the vertical direction, a coma-free image at the entrance slit can be produced. The best monochromators, with regard to resolution, over the desired spectral region, use spherical gratings with incidence angles near normal and equal length of source and objective arms. This configuration greatly reduces coma and other spherical aberrations introduced by the grating surface figure. By considering geometric constraints of the experiment hall along with resolving power, it was decided to utilize the McPherson mount[15] with an optimal focal length of 3.00 m. This mount requires the rotation of the grating while translating it along the bisector of the angle formed by the entrance and exit arms of the reflecting system when the grating is positioned to produce zero-order focus at the exit slit.[16] These two motions are controlled independently by stepping motors. The monocromator is equipped with two interchangeable spherical gratings (from Richardson Grating Laboratory, Rochester, NY) with different blaze angles and surface coatings (see Table I). An ellipsoidal mirror (M_3) focuses the beam exiting the monochromator onto the sample position with a demagnification factor of 0.53. The planes of incidence of all the mirrors and the grating are coincident; the common plane will be termed the plane of incidence of the beamline. The optical design was examined and optimized extensively using the SHADOW ray-tracing calculation package.[17] Theoretical resolving powers and polarizations of the NIM beamline at a few photon energies are given in Table II; these were calculated from information derived by the ray tracing. All major beamline components including mirrors were manufactured by McPherson Inc., Chelmsford, MA.

Because a Scienta electron energy analyzer is permanently placed as an endstation for high-resolution photoemission spectroscopy, a second tail for the beamline was considered to allow a broader range of scientific activity, such as photoionization and photoabsorption spectroscopy of atoms and molecules. The optical design of the second tail is shown in Fig. 2 and the optical parameters are listed in Table III. Due to space limitation around the Scienta endstation, it was not possible to design a single-mirror configuration located near the first tail. The beam, after passing through the exit

a)Author to whom correspondence should be addressed; electronic mail: eizi@lsu.edu

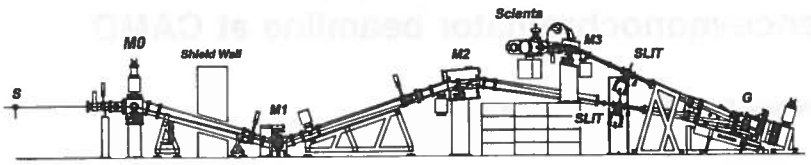

FIG. 1. Layout of the 3 m-NIM beamline at CAMD. The beamline's second tail is not shown here for sake of brevity.

TABLE I. Parameters of the optical components of the 3 m-NIM beamline at CAMD.

M_0	Ellipsoid, copper-alloy, water-cooled, gold-coated, object distance 2800 mm, image distance 11 760 mm, incidence angle 82.5°, size 200 mm wide×200 mm long.
M_1	Cylinder (meridian focus), Zerodur®, gold-coated, radius 3360 mm, incidence angle 73°, size 150×150 mm^2, distance from M_0=3500 mm.
M_2	Bent cylinder, float-glass, radius 16 047 mm, incidence angle 76°, size 90 mm wide and 660 mm long (pole is located 200 mm from upstream edge of mirror), distance from M_1=4449 mm.
G	Spherical grating, radius 2998.3 mm, 1200 g/mm, size 60 mm wide and 110 mm long, Al+MgF_2 overcoat, blaze angle 4.7° (3–12 eV), gold coated, blaze angle 2.0° (10–40 eV).
M_3	Ellipsoid, Zerodur®, gold coated, object distance 1500 mm, image distance 800 mm, incidence angle 78°, size 75 mm wide×190 mm long.

TABLE II. Theoretical resolving power and polarization at exit slit of the 3 m-NIM beamline (calculated with 25 mrad of radiation from CAMD ring).

Energy (eV)	Resolving power 500 μm slits to min	Polarization degree
5	4000–60 000	0.99
7.3	2400–50 000	0.96
15	1100–30 000	0.88
25	700–14 000	0.81
40	500–10 000	0.74

TABLE III. Parameters of the optical components of the second tail.

M_4	Cylinder (tangential focus), retractable, Zerodur®, gold-coated, radius 1322 mm, incidence angle 11°, size 60 mm ×60 mm^2, distance from exit slit 100 cm, image distance 185 cm.
M_5	Toroid, Zerodur®, gold-coated, radius 5531, 371 mm, incidence angle 78°, size 60 mm wide×120 long mm^2, distance from $M4$=300 cm, image distance 115 cm.

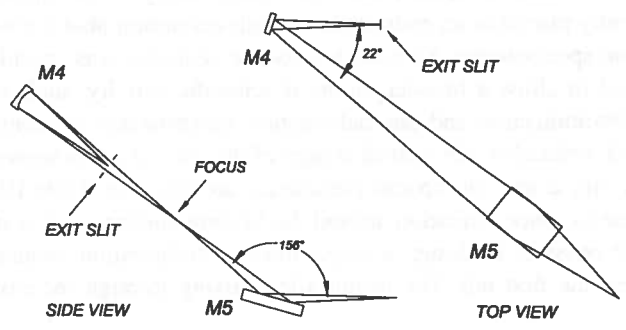

FIG. 2. Optical layout of the second tail of the 3 m-NIM beamline.

slit, is reflected by a (retractable) cylindrical mirror, the incidence angle of this reflection is relatively small and the plane of incidence is orthogonal to the plane of incidence of the (original) beamline. The beam is then reflected up vertically by a toroidal mirror; the output beam is parallel to the floor with a reasonable beam height for most endstations. A total demagnification of 3.48 is achieved in the horizontal direction. In the vertical direction, an intermediate focus is made between the cylindrical and the toroidal mirrors, which allows the use of a relatively small toroidal mirror. The total magnification in the vertical direction is 1.85. Throughput from the second tail is expected to be about 2–3 times less intense than that of the first tail over the range <30 eV, and is about one order of magnitude less for energies >30 eV; attenuation is a result of the extra reflection having a small incidence angle. The radiation densities at the two sample positions (first and second tails) are approximately the same owing to the larger horizontal demagnification of the second tail.

III. PERFORMANCE

The absolute photon flux from the NIM beamline is presented in Fig. 3. Photon intensity at the sample position (entrance and exit slits, 100 μm) was measured by a windowless photodiode (GaAsP, Hamamatsu model 1127-04) with the CAMD ring operated at 1.3 GeV. The measured flux was normalized to ring current of 100 mA and corrected by absolute quantum efficiency of the diode, which has been published.[18] As seen from Fig. 3, accessible energy in the high energy region extends to about 30 eV using the high-energy grating supplied.

A Hg lamp (Pen-Ray lamp No. 90-0012-01, UVP Inc.) was used as a source for evaluating the monochromator resolution as well as accuracy of the wavelength-scan mechanism. In Fig. 4, the width [a full width at half maximum (FWHM)] of a major intense line (2536.5 Å) from the Hg lamp was measured as a function of the monochromator slit

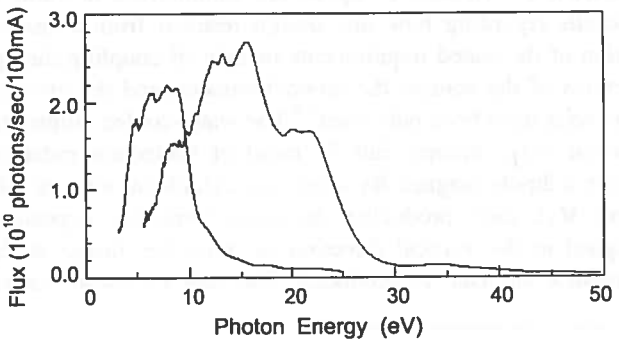

FIG. 3. Measured photon flux at the sample position of the 3 m-NIM beamline (first tail). Left (right) curve corresponds to the low (high) energy grating. Both the entrance and exit slits were set at 100 μm. The flux was normalized to the ring current at 100 mA.

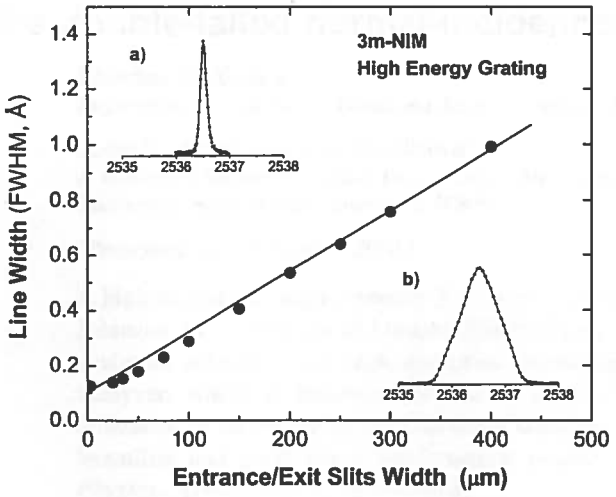

FIG. 4. Width of the Hg-lamp line (2536.5 Å) measured as a function of the monochromator slit widths for the HEG. A Gaussian fit was used to evaluate a FWHM of the measured line width. The linear fit (solid line) extrapolates to 0.10 Å for zero slit width. The measured spectra are shown for 5 μm (a) and for 300 μm (b) widths of the entrance and exit slits.

widths. In general, a spectral linewidth is determined by convolution of the limiting resolution of the monochromator (the instrumental resolution), the bandpass determined by the monochromator slits, and the natural width of the spectral line. By using the zero slit width value (0.10 Å FWHM from extrapolating the plot in Fig. 4) and assuming a natural width of the Hg line as 0.09 Å FWHM, the instrumental resolution is evaluated to be 0.044 Å FWHM at the wavelength of 2536.5 Å (4.89 eV), which corresponds to the resolving power $\lambda/\Delta\lambda = 57\,600$. This obtained instrumental resolving power is in good agreement with the theoretical value listed in Table II.

A very fine step size in scanning the wavelength was realized with the LabView™-based control software provided by McPherson. It was found that the monochromator can be scanned in steps as small as 0.001 Å/step (at 2536.5 Å). However, the scan motion is rather slow and it takes ~4 s/step. Wavelength reproducibility of the monochromator was also evaluated by scanning the Hg line. Several consecutive scans demonstrated very accurate wavelength reproducibility of 0.005 Å (at 2536.5 Å). However, it became worse, 0.058 Å, when the line was scanned after homing the monochromator each time. Since an increment encoder is employed for the wavelength scan motion, a reference position provided by an optical limit switch is needed for a wavelength calibration. Thus, reproducibility of the homing process determines overall accuracy in absolute wavelength of the instrument.

ACKNOWLEDGMENTS

The authors would like to acknowledge extensive technical help for optimization of the monochromator provided by Dr. A. Mihill from McPherson Inc. The operation of CAMD is supported by the State of Louisiana. The NIM beamline was constructed by a grant from the National Science Foundation to a consortium of researchers from the Universities of Tennessee, Texas, Nebraska, Michigan, and the Southern University and the Louisiana State University.

[1] M. Skibowski and W. Steinmann, J. Opt. Soc. Am. **57**, 112 (1967).
[2] V. Saile, Nucl. Instrum. Methods **152**, 59 (1978).
[3] P. R. Woodruff, C. H. Pruett, and F. H. Middleton, Nucl. Instrum. Methods **172**, 181 (1980).
[4] D. L. Ederer, Nucl. Instrum. Methods Phys. Res. **195**, 191 (1982).
[5] V. Saile and J. B. West, Nucl. Instrum. Methods Phys. Res. **208**, 199 (1983).
[6] F. Schafers, W. Peatman, A. Eyers, C. Heckenkamp, G. Schonhense, and U. Heinzmann, Rev. Sci. Instrum. **57**, 1032 (1986).
[7] D. M. P. Holland, J. B. West, A. A. Macdowell, I. H. Munro, and A. G. Beckett, Nucl. Instrum. Methods Phys. Res. B **44**, 233 (1989).
[8] L. R. Hughey, Nucl. Instrum. Methods Phys. Res. A **347**, 294 (1994).
[9] K. Ito, Y. Morioka, M. Ukai, N. Kouchi, Y. Hatano, and T. Hayashi, Rev. Sci. Instrum. **66**, 2119 (1995).
[10] S.-Y. Rah, T.-H. Kang, Y. Chung, B. Kim, and K.-B. Lee, Rev. Sci. Instrum. **66**, 1751 (1995).
[11] R. Reininger, M. C. Severson, R. W. Hansen, W. R. Winter, M. A. Green, and W. S. Tzeciak, Rev. Sci. Instrum. **66**, 2194 (1995).
[12] K. Fukui, H. Nakagawa, I. Shimoyama, K. Nakagawa, H. Okamura, T. Nanba, M. Hasumoto, and T. Kinoshita, J. Synchrotron Radiat. **5**, 836 (1998).
[13] L. Nahon, B. Lagarde, F. Polack, C. Alcaraz, O. Dutuit, M. Vervloet, and K. Ito, Nucl. Instrum. Methods Phys. Res. A **404**, 418 (1998).
[14] E. Morikawa, C. M. Evans, and J. D. Scott, AIP Conf. Proc. **576**, 730 (2001).
[15] J. A. R. Samson, *Techniques of Vacuum Ultraviolet Spectroscopy* (Wiley, New York, 1967), pp. 62–64.
[16] B. R. Lewis, Appl. Opt. **21**, 2523 (1982).
[17] B. Lai, K. Chapman, and F. Cerrina, Nucl. Instrum. Methods Phys. Res. A **266**, 544 (1988).
[18] M. Krumrey, E. Tegeler, J. Barth, M. Krisch, F. Schaefers, and R. Wolf, Appl. Opt. **27**, 4336 (1988).